

Structured-illumination photoacoustic Doppler flowmetry of axial flow in homogeneous scattering media

Ruiying Zhang, Junjie Yao, Konstantin I. Maslov, and Lihong V. Wang

Citation: [Applied Physics Letters](#) **103**, 094101 (2013); doi: 10.1063/1.4819735

View online: <http://dx.doi.org/10.1063/1.4819735>

View Table of Contents: <http://scitation.aip.org/content/aip/journal/apl/103/9?ver=pdfcov>

Published by the [AIP Publishing](#)

Articles you may be interested in

[Pulsed photoacoustic Doppler flowmetry using time-domain cross-correlation: Accuracy, resolution and scalability](#)

J. Acoust. Soc. Am. **132**, 1780 (2012); 10.1121/1.4739458

[Note: Reflection-type micro multipoint laser Doppler velocimeter for measuring velocity distributions in blood vessels](#)

Rev. Sci. Instrum. **82**, 076104 (2011); 10.1063/1.3609864

[Three-dimensional imaging techniques for microvessels using multipoint laser Doppler velocimeter](#)

J. Appl. Phys. **106**, 054701 (2009); 10.1063/1.3211299

[Photoacoustic Doppler flow measurement in optically scattering media](#)

Appl. Phys. Lett. **91**, 264103 (2007); 10.1063/1.2825569

[Transition to turbulence of the flow in a straight pipe downstream of a helical coil](#)

Phys. Fluids **11**, 2993 (1999); 10.1063/1.870158

The advertisement for MMR Technologies features a blue and white background with a grid pattern. On the left is the MMR Technologies logo, which consists of a stylized 'M' and 'R' in blue and red, with 'TECHNOLOGIES' in black below it. To the right of the logo is the text 'THE WORLD'S RESOURCE FOR VARIABLE TEMPERATURE SOLID STATE CHARACTERIZATION' in bold, black, sans-serif font. Below this text are five images of different scientific instruments: a small electronic device, a blue box labeled 'SB1000' and 'K2000', a circular microprobe station, a blue box labeled 'H5000' and 'K2000', and a large cylindrical magnet. At the bottom of the advertisement is the website 'WWW.MMR-TECH.COM' in red, and below it are five labels: 'OPTICAL STUDIES SYSTEMS', 'SEEBECK STUDIES SYSTEMS', 'MICROPROBE STATIONS', 'HALL EFFECT STUDY SYSTEMS AND MAGNETS', and 'K2000'.

Structured-illumination photoacoustic Doppler flowmetry of axial flow in homogeneous scattering media

Ruiying Zhang,^{a)} Junjie Yao,^{a)} Konstantin I. Maslov, and Lihong V. Wang^{b)}

Optical Imaging Laboratory, Department of Biomedical Engineering, Washington University in St. Louis, One Brookings Dr., St. Louis, Missouri 63130, USA

(Received 3 July 2013; accepted 15 August 2013; published online 28 August 2013)

We propose a method for photoacoustic flow measurement based on the Doppler effect from a flowing homogeneous medium. Excited by spatially modulated laser pulses, the flowing medium induces a Doppler frequency shift in the received photoacoustic signals. The frequency shift is proportional to the component of the flow speed projected onto the acoustic beam axis, and the sign of the shift reflects the flow direction. Unlike conventional flowmetry, this method does not rely on particle heterogeneity in the medium; thus, it can tolerate extremely high particle density. A red-ink phantom flowing in a tube immersed in water was used to validate the method in both the frequency and time domains. The phantom flow immersed in an intralipid solution was also measured. © 2013 AIP Publishing LLC. [<http://dx.doi.org/10.1063/1.4819735>]

Flow speed measurement plays an important role in biomedical research, such as the study of tumor and cardiovascular diseases.^{1–3} In biomedical imaging, Doppler ultrasound flowmetry,^{4,5} laser Doppler flowmetry⁶ and Doppler optical coherence tomography⁷ are all valuable tools for flow speed measurement. However, based on backscattered signals, these Doppler techniques require particle heterogeneity in the flowing medium;^{4–7} thus, they cannot be used for flow measurement of a homogeneous medium. In comparison, photoacoustic imaging, based on optical absorption contrast,⁸ is not intrinsically limited by the heterogeneity of the flowing medium. A few recent studies have investigated photoacoustic Doppler (PAD) flowmetry of particle-based phantoms.^{9–16} It has been reported that the traditional PAD signal strength decreases and eventually diminishes as the particle concentration increases.^{17,18} In this paper, we propose a flow measurement method based on the PAD effect in homogeneous media, where the distance between absorptive molecules is on the scale of nanometers. Different from traditional PAD implementations, which use a temporally modulated CW or tone-burst laser excitation, our method uses a spatially modulated pulsed laser excitation to temporally modulate the received PA signals. The modulation frequency of the received PA signals is determined by the acoustic transit time between the neighbouring pitches of the spatial modulation. Therefore, the flow of the medium changes the acoustic transit time and thus induces a frequency shift in the received PA signals. As in traditional PAD flow measurement,^{9–16} the flow direction determines the sign of the frequency shift.

In PA flow measurement of a homogeneous medium, a stationary ultrasonic detector receives signals from the excited region of the medium, which is the acoustic source. As shown in Figure 1(a), if both the acoustic source and the medium are stationary, the PA wave from the stationary

acoustic source travels to the transducer surface at the speed of sound in the medium (~ 1480 m/s in water at 20°C). If both the acoustic source and the medium are moving, the received PA signal will be compressed or stretched, depending on the flow direction. In the time domain, this compressing or stretching effect can be further decomposed into two parts: the arrival time shift induced by the moving medium and the signal duration scaling induced by the moving source. In the frequency domain, while the arrival time shift corresponds to the phase shift at each frequency, the signal duration scaling corresponds to the scaling of the frequency spectrum. Both the arrival time shift and the signal duration scaling can be used to measure flow speed. However, using the arrival time shift requires exact knowledge of the sound path between the acoustic source and the transducer, which is challenging to achieve in biological tissues. By contrast, the signal duration scaling relies only on the acoustic property of the moving source, even if the sound path between the source and ultrasonic transducer is uncertain. In this study, we explored four methods of PAD flowmetry of homogeneous media: (1) central frequency shift; (2) arrival time shift; (3) phase change at each frequency; and (4) temporal scaling.

Central Frequency Shift: Similar to traditional PAD flow measurement, if the PA signal generated by the moving source has a central frequency with a narrow bandwidth, then the scaling of the spectrum can be represented by its central frequency shift, from which the medium's flow speed and direction can be derived. In our method, the modulation frequency f_0 can be estimated as

$$f_0 = v_a/d_0, \quad (1)$$

where v_a is the speed of sound in the stationary medium and d_0 is the fringe pitch of the spatially modulated illumination.

Then, the central frequency shift can be expressed as

$$f_{PAD} = f_0 \frac{v_m}{v_a}, \quad (2)$$

^{a)}R. Zhang and J. Yao contributed equally to this work.

^{b)}Author to whom correspondence should be addressed. Electronic mail: lhwang@biomed.wustl.edu

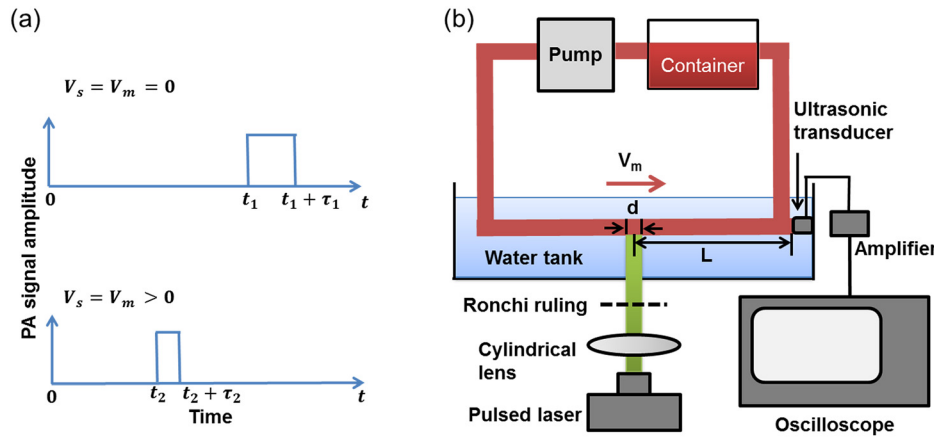


FIG. 1. Flow measurement based on the PAD effect in a homogeneous medium. (a) Schematic of PA signals under different flow conditions. v_s and v_m are the flow speeds of the source and the medium, respectively; t_1 and t_2 are the arrival times of signals under the two flow conditions; τ_1 and τ_2 are the signal durations under the two flow conditions. Both the arrival time and the signal duration decrease when $v_s = v_m > 0$ (flow is towards the transducer), compared with when $v_s = v_m = 0$. (b) Schematic of experimental setup. The homogenous flow with speed v_m is excited by structured illumination, and the generated PA signal is detected by a flat ultrasonic transducer placed in the axial direction of the tube. L is the distance between the illumination spot and the transducer surface, and d is the illumination spot size.

where v_m is the flow speed of the medium projected along the acoustic beam axis. A positive frequency shift means the medium is flowing towards the transducer, and vice versa. Note that the PAD frequency shift in Eq. (2) is only half of the traditional ultrasound Doppler shift, due to the one-way emission of the PA signals. In practice, the central frequency of the PA signal can be estimated as the power-weighted mean frequency.^{19,20}

Arrival Time Shift: This method is predicated on the assumption that both the flow speed and acoustic property along the path are uniform. The time shift Δt_m can be estimated by cross-correlation between the received PA signal $p_1(t)$ at flow speed v_1 and the PA signal $p_0(t)$ at a baseline flow speed v_0 . If the flight time of the signal is much longer than its duration (i.e., the distance from the center of the illumination spot to the transducer is much larger than the size of the illumination spot), the contribution of the signal duration to the cross-correlation can be neglected. Thus, by finding the time delay Δt_m that maximizes the cross-correlation between $p_1(t)$ and $p_0(t)$, the relative flow speed Δv_m can be calculated as follows:

$$\Delta t_m = \underset{\Delta t}{\operatorname{argmax}} \int_0^{t_{\max}} p_0(t) p_1(t + \Delta t) dt, \quad (3)$$

$$\Delta v_m = v_a^2 \frac{\Delta t_m}{L}, \quad (4)$$

where t_{\max} represents the ending point of the signal and L is the distance between the transducer and the center of the illumination spot. A positive arrival time shift means the medium is flowing away from the transducer, and vice versa.

Phase Change: Alternatively, in the frequency domain, the phase information of the cross-spectral density function of the signal can also be used to calculate the time delay Δt_m .²¹ We have

$$\Delta t_m = \frac{1}{2\pi f} \operatorname{arg} S_{p_1 p_0}(f), \quad (5)$$

where $S_{p_1 p_0}(f)$ is the cross-spectral density of the received signals $p_1(t)$ and $p_0(t)$. After extracting the phase from $S_{p_1 p_0}(f)$, we can then fit for the arrival time shift Δt_m using Eq. (5) and calculate the flow speed using Eq. (4).

Temporal Scaling: In the time domain, in addition to the approximate calculation method based on cross-correlation, the flow speed can also be estimated by a more accurate temporal scaling method. The scaling factor ε_m that maximizes the product of $p_1(\varepsilon_m t)$ and $p_0(t)$ can be calculated using Eq. (6), and the flow speed is given by Eq. (7)

$$\varepsilon_m = \underset{\varepsilon}{\operatorname{argmax}} \int_0^{t_{\max}} p_0(t) p_1(\varepsilon t) dt, \quad (6)$$

$$\Delta v_m = (1 - \varepsilon_m) v_a. \quad (7)$$

A temporal scaling factor less than one means the medium is flowing towards the transducer, and vice versa.

Here, photoacoustic flow sensing based on the PAD effect from a homogeneous medium was demonstrated in a laboratory setup, shown in Fig. 1(b). A pump (Model 3386, Fisher Scientific and EW-72008-00, Cole Parmer) drove the flow in a clear polyvinyl chloride tube (ClearFlexTM 60 premium, 8 mm inner diameter) immersed in water. Nanosecond laser pulses of 570 nm wavelength were focused by a cylindrical lens (300 mm focal length), which generated a 3-mm-long illumination line along the tube axis. A Ronchi ruling (50 μm pitch size) was placed above the tube, which provided a spatial modulation of the illumination intensity. A diluted red ink solution (optical absorption coefficient: $\mu_a \approx 1.2 \text{ cm}^{-1}$) was used as the flowing medium. The generated photoacoustic waves propagated in the flowing medium and were detected by a flat ultrasonic transducer (V2022 BC, Olympus-NDT). The distance between the illumination spot and the transducer surface was approximately 5.6 cm. The PA signals from the transducer were amplified by 40 dB and then sampled by an oscilloscope (TDS5034, Tektronix, Inc.). The recorded PA signals were averaged for 256 times. In a second experiment with a scattering medium, the tube was immersed in a 0.1% intralipid solution (optical scattering coefficient: $\mu_s \approx 6.18 \text{ cm}^{-1}$ at 570 nm).²²

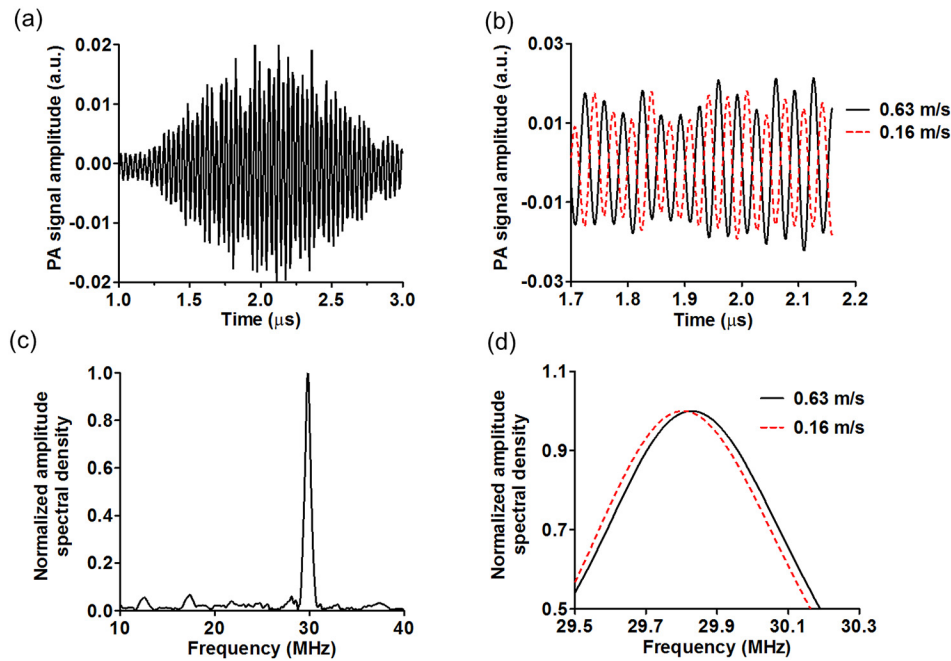


FIG. 2. Representative PA signals in the time and frequency domains. The laser spot size was 3 mm, and the distance from the transducer surface to illumination spot was 5.6 cm. (a) Representative time-domain PA signal with zero flow speed, where the signal modulation is induced by the Ronchi ruling. (b) Close-up of the PA signals at flow speeds of $v_1 = 0.63$ m/s and $v_2 = 0.16$ m/s. (c) Representative PA signal spectrum at flow speed $v_1 = 0.63$ m/s with a central frequency at 29.8 MHz. (d) Close-up of the frequency spectra at flow speeds $v_1 = 0.63$ m/s and $v_2 = 0.16$ m/s.

Fig. 2(a) shows the temporal profile of a typical photoacoustic signal from a stationary homogeneous medium, where the signal modulation is clear. The arrival time was about $37.5 \mu\text{s}$, which corresponded to a distance of ~ 5.6 cm between the illumination spot and the transducer surface. The total duration of the signal was about $2 \mu\text{s}$, which corresponded to an illumination spot size of ~ 3 mm. As shown in Fig. 2(b), a faster flow (0.63 m/s) of the medium towards the transducer induces a shorter arrival time of the signal than a slower flow (0.16 m/s), producing a time shift in the temporal profile of the received PA signal. Correspondingly, Fig. 2(c) shows the frequency spectrum of the PA signal acquired at a flow speed of 0.63 m/s. The signal has a central frequency of 29.8 MHz with a full-width at half maximum of 9.7 MHz. According to Eq. (2), the central frequency is related to the spatial modulation

frequency of the illumination pattern, the propagation speed of sound in the homogeneous medium. The bandwidth is determined by the duration of the PA signal, which is also related to the propagation speed of sound in the medium. A faster flow of the medium towards the transducer shortens the signal duration and increases the central frequency of the received PA signal, as shown in Fig. 2(d).

In the first experiment, with the tube immersed in water, the flow speed of the ink solution was varied from 0.020 m/s to 1.4 m/s. The four methods introduced above were used to calculate the flow speeds. As shown in Fig. 3, the measurements from all four methods agree well with the preset speeds. The root-mean-square-errors (RMSE) of the four methods were 0.089 m/s, 0.095 m/s, 0.10 m/s, and 0.057 m/s, respectively.

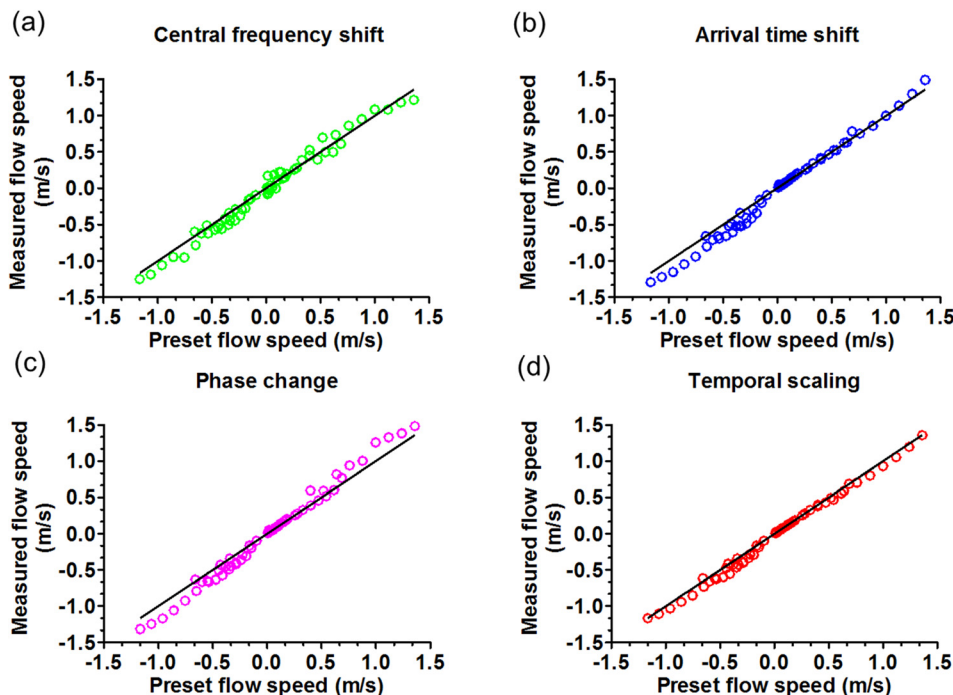


FIG. 3. Flow speed measurements in a clear medium, based on four different methods. Solid lines: $y = x$. (a) Flow speed measurement based on central frequency shift, with $RMSE = 0.089$ m/s. (b) Flow speed measurement based on arrival time shift, with $RMSE = 0.095$ m/s. (c) Flow speed measurement based on phase change versus frequency, with $RMSE = 0.10$ m/s. (d) Flow speed measurement based on temporal scaling, with $RMSE = 0.057$ m/s.

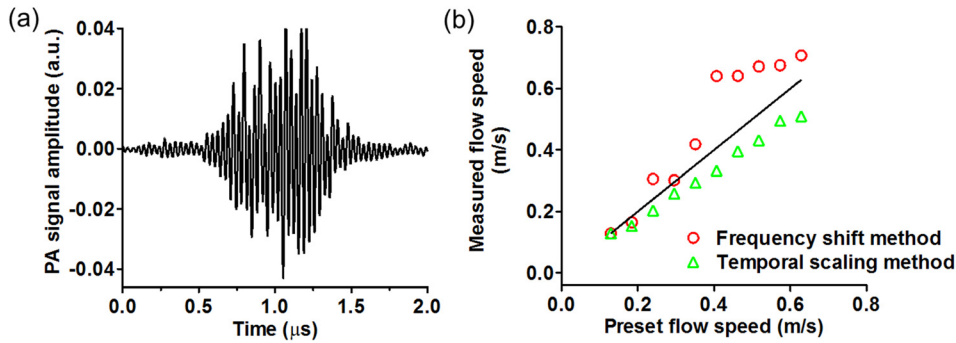


FIG. 4. Photoacoustic flow measurement in a 0.1% intralipid solution. (a) PA signal in the time domain. (b) Flow speed measurements based on the central frequency shift method and temporal scaling method, with RMSE = 0.12 m/s and 0.066 m/s, respectively. Solid line: $y = x$.

In addition to the clear medium, PA flow measurements were also demonstrated in an intralipid scattering medium. The intralipid solution above the tube surface was ~ 3 mm thick. The flow speed was varied from 0.13 m/s to 0.63 m/s. The temporal scaling method and the central frequency shift method were used for flow speed quantification, as shown in Fig. 4. Compared with the measurements in the clear medium, the measured flow speeds in the scattering medium had greater errors for both methods. For the time domain method, optical scattering reduced the signal-to-noise ratio (SNR), which resulted in a greater error in the temporal scaling measurement (RMSE: 0.066 m/s). For the frequency domain method, in addition to the reduced SNR, the scattering also degraded the PA signal modulation depth, thereby increasing the difficulty in measuring the central frequency (RMSE: 0.12 m/s).

Based on the translation and scaling properties of the Fourier transformation, the time shift in the time domain is equivalent to the phase shift in the frequency domain, and scaling in the time domain is equivalent to scaling in the frequency domain. Nevertheless, superior to the other three methods, the central frequency shift method can sense the absolute flow speed instead of a relative flow speed. Furthermore, the central frequency shift method does not assume uniform flow and homogeneous acoustic property along the sound path between the laser spot and the transducer surface. Instead, it requires only uniformity within the illumination spot, which is much easier to satisfy in practice.

It should be noted that the proposed method assumes a uniform flow speed over the depth direction of the tube that the laser can penetrate. However, this is not true for laminar flow, where the center of the tube has the fastest flow. For the absorption coefficient of the ink solution, the $1/e$ penetration depth of the light was approximately 8.3 mm, larger than the tube diameter. Therefore, the measured flow speed was an average of the actual flow distribution.

The modulated light illumination provides a central frequency for the received PA signal, which can help quantify the absolute flow speed. It transforms the otherwise wideband PA signal into a narrowband signal. Without the light modulation, the wideband spectrum would be compressed or stretched as well, depending on the flow direction. The scaling factor can also be used to estimate flow; however, it can detect only relative flow speeds.

In the central frequency shift method, the maximum measurable flow speed is limited by the frequency response of the transducer and SNR. Assuming the maximum frequency

response of the transducer is ~ 105 MHz, the maximum measurable flow speed is ~ 3700 m/s (flow is towards the transducer), using Eq. (2). Increasing the bandwidth of the transducer can increase the maximum measurable flow speed. However, since the acoustic signal is attenuated more at higher frequencies, higher frequency components have lower SNR, which will limit the maximum measurable flow speed.

The minimum measurable flow speed, which is the velocity sensitivity of the system, is limited by the signal length and SNR. Increasing the cycle number of the Ronchi ruling can improve the frequency resolution, and thus decrease the minimum measurable flow speed. In addition, zero-padding can be used in the Fourier transformation to improve flow sensitivity. While zero-padding cannot actually improve the frequency resolution, it can smooth the frequency spectrum and thus improve the accuracy of locating the central frequency.²³ If the noise is spectrally white, the minimum measurable flow speed can be derived from the Cramér–Rao lower bound, which gives an estimation accuracy of the central frequency as^{24,25}

$$\sigma_f^2 = \frac{3f_s^2}{\pi^2 N(N^2 - 1)SNR}, \quad (8)$$

$$v_{\min} = 2\sigma_f v_a / f_0, \quad (9)$$

where σ_f is the standard deviation of the central frequency computed from the measured PA spectrum, f_s is the sampling frequency, N is the number of sampling points, f_0 is the modulation frequency, v_a is the speed of sound within the medium, and $SNR = A^2 / 2\sigma_n^2$ (A is amplitude of the signal and σ_n^2 is the variance of the noise). In our experiment, given $SNR = 10000$, $N = 10^4$, and $f_s = 2.5$ GHz, we get $v_{\min} = 0.014$ m/s.

In conclusion, we have proposed a flow speed measurement method based on the photoacoustic Doppler effect in a homogeneous medium. Unlike the back-scattering based Doppler method, our method does not require heterogeneity of the flowing medium on the scale of the spatial resolution. As long as the medium is optically absorptive at a certain wavelength, such as pure water in the infrared region, its flow speed can be measured based on the photoacoustic Doppler effect. Although we emphasized the central frequency shift method, the other three methods can also be utilized for relative flow speed calculation. While the current experimental setup is more suitable for fast flow (> 2.0 cm/s) measurement, the slow flow measurement capability can be improved, for example, by increasing the modulation frequency.

The authors would like to thank Professor James Ballard for his close reading of the manuscript. We also appreciate technical assistance from and useful discussions with Lidai Wang, Yong Zhou, Jinyang Liang, Wenxin Xing, Arie Krumholz, and Yan Liu. This research was supported by the National Institutes of Health Grants DP1 EB016986 (NIH Director's Pioneer Award), R01 EB008085, R01 CA134539, U54 CA136398, R01 CA157277, R01 CA159959. L.V.W. has a financial interest in Microphotoacoustics, Inc. and Endra, Inc., which, however, did not support this work. K.M. has a financial interest in Microphotoacoustics, Inc., which, however, did not support this work.

- ¹W. W. Nichols, M. F. O'Rourke, and C. Vlachopoulos, *McDonald's Blood Flow in Arteries: Theoretical, Experimental and Clinical Principles* (CRC Press, Boca Raton, 2011), pp. 1–12.
- ²K. K. Shung, *Diagnostic Ultrasound: Imaging and Blood Flow Measurements* (CRC Press, Boca Raton, 2005), pp. 1–2.
- ³R. J. Goldstein, *Fluid Mechanics Measurements* (CRC Press, Boca Raton, 1996), pp. 2–3.
- ⁴D. N. White, *Ultrasound Med. Biol.* **8**(6), 583 (1982).
- ⁵D. Evans and W. McDicken, *Doppler Ultrasound: Physics, Instrumentation and Signal Processing*, 2nd ed. (Wiley, Chichester, 2000), pp. 204–207.
- ⁶P. A. Oberg, *Crit. Rev. Biomed. Eng.* **18**(2), 125 (1990).
- ⁷C. Zhongping, Y. Zhao, S. M. Srinivas, J. S. Nelson, N. Prakash, and R. D. Frostig, *IEEE J. Sel. Top. Quantum Electron.* **5**(4), 1134 (1999).

- ⁸L. V. Wang and S. Hu, *Science* **335**(6075), 1458 (2012).
- ⁹J. Yao and L. V. Wang, *J. Biomed. Opt.* **15**(2), 021304 (2010).
- ¹⁰J. Yao, K. I. Maslov, Y. Zhang, Y. Xia, and L. V. Wang, *J. Biomed. Opt.* **16**(7), 076003 (2011).
- ¹¹A. Sheinfeld, S. Gilead, and A. Eyal, *J. Biomed. Opt.* **15**(6), 066010 (2010).
- ¹²A. Sheinfeld, S. Gilead, and A. Eyal, *Opt. Express* **18**(5), 4212 (2010).
- ¹³H. Fang, K. Maslov, and L. V. Wang, *Appl. Phys. Lett.* **91**(26), 264103 (2007).
- ¹⁴H. Fang, K. Maslov, and L. V. Wang, *Phys. Rev. Lett.* **99**(18), 184501 (2007).
- ¹⁵J. Brunker and P. Beard, *J. Acoust. Soc. Am.* **132**(3), 1780 (2012).
- ¹⁶J. Brunker and P. Beard, *Proc. SPIE* **7564**, 756426–756433 (2010).
- ¹⁷J. Yao, K. I. Maslov, Y. Shi, L. A. Taber, and L. V. Wang, *Opt. Lett.* **35**(9), 1419 (2010).
- ¹⁸P. Beard, *Interface Focus* **1**(4), 602 (2011).
- ¹⁹N. T. Ursem, H. J. Brinkman, P. C. Struijk, W. C. Hop, M. H. Kempster, B. B. Keller, and J. W. Wladimiroff, *Ultrasound Med. Biol.* **24**(1), 1 (1998).
- ²⁰K. L. Fernando, V. J. Mathews, and E. B. Clark, *IEEE Signal Process. Lett.* **11**(2), 175 (2004).
- ²¹K. Shin and J. Hammond, *Fundamentals of Signal Processing for Sound and Vibration Engineers* (Wiley, San Francisco, 2008), pp. 267–270.
- ²²H. J. van Staveren, C. J. M. Moes, J. van Marie, S. A. Pahl, and M. J. C. van Gemert, *Appl. Opt.* **30**(31), 4507 (1991).
- ²³S. M. Kay and S. L. Marple, Jr., *Proc. IEEE* **69**(11), 1380 (1981).
- ²⁴D. Rife and R. Boorstyn, *IEEE Trans. Inf. Theory* **20**(5), 591 (1974).
- ²⁵H.-E. Albrecht, *Laser Doppler and Phase Doppler Measurement Techniques* (Springer Verlag, New York, 2003), pp. 290–300.